



HAL
open science

Robust and direct evaluation of $J(2)$ in linear elastic fracture mechanics with the X-FEM

Grégory Legrain, Nicolas Moes, Erwan Verron

► **To cite this version:**

Grégory Legrain, Nicolas Moes, Erwan Verron. Robust and direct evaluation of $J(2)$ in linear elastic fracture mechanics with the X-FEM. *International Journal for Numerical Methods in Engineering*, 2008, 76 (10), pp.1471-1488. 10.1002/nme.2366 . hal-01007266

HAL Id: hal-01007266

<https://hal.science/hal-01007266>

Submitted on 16 Jun 2014

HAL is a multi-disciplinary open access archive for the deposit and dissemination of scientific research documents, whether they are published or not. The documents may come from teaching and research institutions in France or abroad, or from public or private research centers.

L'archive ouverte pluridisciplinaire **HAL**, est destinée au dépôt et à la diffusion de documents scientifiques de niveau recherche, publiés ou non, émanant des établissements d'enseignement et de recherche français ou étrangers, des laboratoires publics ou privés.



Distributed under a Creative Commons Attribution 4.0 International License

Robust and direct evaluation of J_2 in linear elastic fracture mechanics with the X-FEM

G. Legrain, N. Moës and E. Verron

*GeM Institute—Ecole Centrale de Nantes, Université de Nantes, CNRS, 1 Rue de la Noë,
BP92101, 44321 Nantes, France*

The aim of the present paper is to study the accuracy and the robustness of the evaluation of J_k -integrals in linear elastic fracture mechanics using the extended finite element method (X-FEM) approach. X-FEM is a numerical method based on the partition of unity framework that allows the representation of discontinuity surfaces such as cracks, material inclusions or holes without meshing them explicitly. The main focus in this contribution is to compare various approaches for the numerical evaluation of the J_2 -integral. These approaches have been proposed in the context of both classical and enriched finite elements. However, their convergence and the robustness have not yet been studied, which are the goals of this contribution. It is shown that the approaches that were used previously within the enriched finite element context do not converge numerically and that this convergence can be recovered with an improved strategy that is proposed in this paper.

KEY WORDS: partition of unity; linear fracture mechanics; extended finite element method; vectorial J -integral

1. INTRODUCTION

The numerical simulation of fracture mechanics is of major importance in the design of structures such as aircrafts or dams. For complex structures, robustness and accuracy of predictions are essential pre-requisites to use numerical methods for new parts design. The finite element method (FEM) is classically considered for the simulation of such problems. However, cracks must be explicitly meshed in order to incorporate the discontinuity of the displacement field across their faces. In addition, this process has to be handled at each step of propagation of the cracks. The main drawback of this approach is the computational and human cost of remeshing. Nevertheless, numerical tools improved much over the past years. Meshless methods (such as EFGM [1] or

hp-clouds [2]) were proposed to avoid meshing of the domain studied and to improve the quality of the results by enriching the approximation. FEMs were also thoroughly improved using the concept of partition of unity [3], which was first employed in the context of meshless methods by Oden and Duarte [2, 4]. Among the class of partition of unity FEMs, the generalized finite element method (GFEM) and the extended finite element method (X-FEM) are the most advanced. The GFEM was introduced by Strouboulis *et al.* [5, 6] and was applied to the simulation of problems with complex micro-structures (see also the work of Babuška *et al.* [7] and Oden *et al.* [8]). The method was further extended to employ the idea of mesh-based numerically constructed handbook functions by Strouboulis *et al.* [9, 10].

Concerning the X-FEM, it was first proposed as a solution to the remeshing issue for crack propagation in linear elastic fracture mechanics [11, 12]. It uses the partition of unity in two ways: first to take into account the displacement jump across the crack faces far away from the crack tip and second to enrich the approximation with analytical asymptotic fields close to the tip. Many fracture mechanics problems have been successfully solved with the X-FEM approach: 2D [12–16], 3D [17–20], plates and shells [21–23], cohesive zone modelling [24, 25], dynamic fracture [26], non-linear fracture mechanics [27–31] among others. For a wider review on partition of unity finite elements applied to fracture mechanics, the reader could also refer to [32].

A major issue in fracture mechanics is the prediction of crack kinking. In order to predict crack growth direction, several criteria have been proposed: one can cite, for example, the maximum hoop stress criterion [33], the maximum tangential stress criterion or the symmetry principle [34]. The maximum energy release rate criterion [35], also called as the ‘vectorial J -integral’ criterion [36], is an alternative, which was initially proposed by Hellen and Blackburn [36]. The main difference in evaluating this criterion with respect to the classical J -integral relies on the difficulties in the evaluation of the second component J_2 of the energy release rate vector \mathbf{J} . It is well known that J_1 (which is basically the J -integral) is path-independent. Concerning J_2 , Herrmann and Herrmann [37] have shown that it is path-independent only in a modified manner, i.e. by adding an extra contribution on the crack faces. However, this new contribution requires an accurate determination of the mechanical fields near the crack tip. It is well known that the quality of these fields near a singularity is not ensured in the finite element context. This is why some authors proposed specific strategies for an accurate numerical evaluation of J_2 . The pioneering contribution is by Eischen [38] who proposed to decompose the integration into two parts: The first one far from the tip, evaluated using finite elements, and the second one close from the crack tip, calculated using near-tip asymptotic fields. Evaluating two contour integrals, it is then possible to calculate J_2 . One drawback of this approach is that it involves contour integrals, which are not well-adapted to finite elements. This contrasts with the evaluation of the J -integral that can be performed considering a domain integral by means of a virtual velocity field [39]. This is why Chang and Yeh [40] proposed an approach similar to that in [38], but with the use of domain integrals.

For enriched FEMs, the only study on this subject was recently proposed by Heintz [41] in the context of configurational forces. His approach is directly related to the one proposed in [40], except that no decomposition of the integral is considered to avoid the near-tip integration. The major advantages of this direct approach are that it does not necessitate near-tip fields assumptions and that it requires only one computation of the domain integral.

The accurate prediction of the crack kinking angle highly depends on the accuracy and robustness of the \mathbf{J} -integral calculation. Nevertheless, no study has been proposed to evaluate the accuracy of the above-mentioned methods. This contrasts with the numerical evaluation of stress intensity factors within X-FEM, which has already been investigated in 2D and 3D [19, 20, 23, 42].

The aim of the present paper is to compare various numerical approaches for the evaluation of the **J**-integral. It will be demonstrated that some of these approaches do not converge. Improvements will be proposed in order to overcome the lack of convergence.

This paper is organized as follow. First, the governing equations are presented. Then, X-FEM basics are recalled. The third section presents the classical approaches used to compute the **J**-integral; finally, a new method is proposed in order to ensure convergence of the calculation.

2. GOVERNING EQUATIONS

Consider the static response of a 2D cracked elastic body that occupies a bounded domain Ω with a sufficiently smooth boundary $\partial\Omega$ split into two disjoint parts: $\partial\Omega_u$ where displacements are prescribed (Dirichlet boundary conditions) and $\partial\Omega_t$ where tractions are prescribed (Neumann boundary conditions) (see Figure 1); $\partial\Omega_t$ includes the crack Γ_C . The body is initially in an undeformed and stress-free configuration. The governing equations are as follows:

$$\begin{aligned} \text{div}\underline{\underline{\sigma}} + \mathbf{b} &= \mathbf{0} \quad \text{in } \Omega \\ \underline{\underline{\varepsilon}} &= \frac{1}{2}(\underline{\underline{\nabla}}\mathbf{u} + \underline{\underline{\nabla}}\mathbf{u}^T) \quad \text{in } \Omega \\ \underline{\underline{\sigma}} \cdot \mathbf{n} &= \mathbf{T}_d \quad \text{on } \partial\Omega_t \\ \mathbf{u}(\mathbf{x}) &= \mathbf{u}_d \quad \text{on } \partial\Omega_u \\ \underline{\underline{\sigma}} &= \mathcal{C} : \underline{\underline{\varepsilon}} \quad \text{in } \Omega \end{aligned} \tag{1}$$

where $\underline{\underline{\sigma}}$ is the Cauchy stress tensor, \mathbf{b} is the body force, \mathbf{u}_d is the prescribed displacement field, \mathbf{T}_d are the prescribed tractions, \mathbf{n} is the outward unit normal to the boundary $\partial\Omega$, $\underline{\underline{\varepsilon}}$ is the linearized strain tensor and \mathcal{C} is the fourth-order elasticity tensor. For a linear isotropic elastic material, the constitutive equation depends only on two scalar parameters λ and μ (the Lamé coefficients) and can be expressed as

$$\underline{\underline{\sigma}} = \lambda \text{Tr}(\underline{\underline{\varepsilon}}) \mathbf{I} + 2\mu \underline{\underline{\varepsilon}}(\mathbf{u}) \tag{2}$$

The above strong form of the governing equation (1) can be expressed into the following weak form:

$$\int_{\Omega} \delta \mathbf{u} \cdot \mathbf{b} dV + \int_{\partial\Omega_t} \delta \mathbf{u} \cdot \mathbf{T}_d dA = \int_{\Omega} \delta \underline{\underline{\varepsilon}}(\mathbf{u}) : \underline{\underline{\sigma}} dV \quad \forall \delta \mathbf{u} \in H^1(\Omega) | \delta \mathbf{u} = \mathbf{0} \text{ on } \partial\Omega_u \tag{3}$$

3. THE X-FEM

The above weak formulation (3) will be numerically solved considering the approximation of displacement and test fields. With classical finite elements, the approximation of a vector field $\mathbf{u}(\mathbf{x})$ on an element Ω_e is given as

$$\mathbf{u}(\mathbf{x})|_{\Omega_e} = \sum_{\alpha=1}^n u^{\alpha} \mathbf{N}^{\alpha}(\mathbf{x}) \tag{4}$$

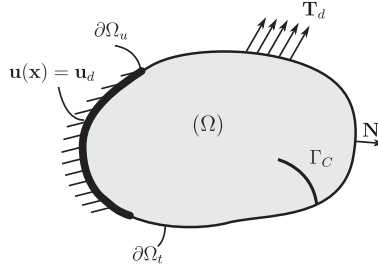


Figure 1. Deformation of a cracked body.

where n is the number of coefficients describing the approximation over the element, u^α is the α th nodal value of this approximation and \mathbf{N}^α is the classical vectorial shape function associated with the degree of freedom (dof) u^α . Within the partition of unity, the approximation can be enriched as

$$\mathbf{u}(\mathbf{x})|_{\Omega_e} = \sum_{\alpha=1}^n \mathbf{N}^\alpha \left(u^\alpha + \sum_{\beta=1}^{n_e} a_\beta^\alpha \phi_\beta(\mathbf{x}) \right) \quad (5)$$

where n_e is the number of enrichment modes, a_β^α is the additional dof associated with dof α and ϕ_β stands for the β th scalar enrichment function. Two different enrichments are considered in fracture mechanics [11, 12]:

- The first enrichment is a discontinuous enrichment for nodes whose support is bisected by the crack. In this case, the interpolation of the displacement field is discontinuous across the crack faces. A Heaviside jump function is considered to model this discontinuity: it equals $+1$ on one side of the crack and -1 on the other side. The associated dof manages the magnitude of the displacement discontinuity. The Heaviside function is computed using the level set representation of the crack [17, 43].
- The second enrichment is a near-tip enrichment for nodes whose support contains the crack tip. In linear elastic fracture mechanics, these enrichment functions are determined using the asymptotic displacement field near the tip of the crack.

$$\phi(r, \theta) = \left\{ \sqrt{r} \sin \frac{\theta}{2}, \sqrt{r} \cos \frac{\theta}{2}, \sqrt{r} \sin \frac{\theta}{2} \sin(\theta), \sqrt{r} \cos \frac{\theta}{2} \sin(\theta) \right\} \quad (6)$$

Finally, it is important to note that the modified Gauss quadrature scheme described in [12] is used to integrate both discontinuous and non-polynomial functions over the elements. For a more detailed presentation of fracture mechanic applications within X-FEM, the reader can refer to [12, 17, 18, 43–45].

4. NUMERICAL EVALUATION OF THE VECTORIAL J -INTEGRAL

In this section, the definition of the \mathbf{J} -integral is first recalled. Then, strategies are presented in order to numerically evaluate this quantity. Next, attention is paid to the accuracy of these approaches in the context of enriched FEMs.

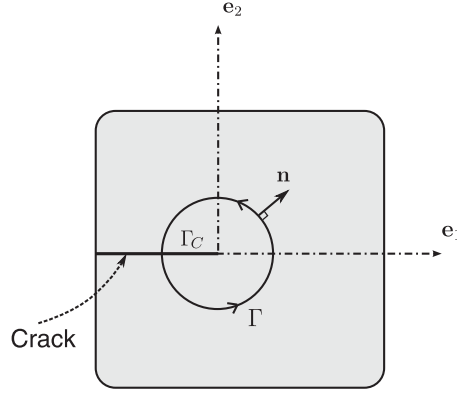


Figure 2. Definitions for the \mathbf{J} -integral.

4.1. \mathbf{J} and $(J_k)_{k=1,2}$ integrals

Consider a 2D cracked body and the crack local coordinate system $(\mathbf{e}_1, \mathbf{e}_2)$ as depicted in Figure 2. Consider a contour Γ that encloses the crack tip and \mathbf{n} denotes its unit outward normal. The J -integral is defined as [46]

$$J = \int_{\Gamma \rightarrow 0} \left(W n_1 - \sigma_{ij} n_j \left(\frac{\partial u_i}{\partial x_1} \right) \right) d\Gamma \quad (7)$$

where n_1 is the projection of \mathbf{n} on \mathbf{e}_1 and W is the strain energy density of the material. This integral is a contour integral that was seen to be path-independent [46]. A second integral called J_2 can be introduced such that both J_k ($k=1, 2$) integrals are defined as

$$J_k = \int_{\Gamma \rightarrow 0} \left(W n_k - \sigma_{ij} n_i \left(\frac{\partial u_i}{\partial x_k} \right) \right) d\Gamma \quad (8)$$

$$= \int_{\Gamma \rightarrow 0} \underline{\underline{\mathbf{M}}} \cdot \mathbf{n} d\Gamma \cdot \mathbf{e}_k \quad (9)$$

where $\underline{\underline{\mathbf{M}}} = W \underline{\underline{\mathbf{I}}} - \underline{\underline{\nabla}} \mathbf{u}^T \underline{\underline{\sigma}}$ is the Eshelby stress tensor [47]. Using this expression, the J -integral is the first component of a vector \mathbf{J} whose components on $(\mathbf{e}_1, \mathbf{e}_2)$ are J_1 and J_2 , respectively. J_2 is not path-independent. Nevertheless, it is said to be path-independent in a modified sense [38]: If Γ does not tend to the tip anymore, an extra boundary term has to be taken into account on the crack faces, and \mathbf{J} can be expressed as

$$\mathbf{J} = \int_{\Gamma} \underline{\underline{\mathbf{M}}} \cdot \mathbf{n} d\Gamma + \int_{\Gamma_C} \llbracket W \rrbracket \mathbf{n} d\Gamma \quad (10)$$

where $\llbracket W \rrbracket$ stands for the jump in the strain energy density across the crack faces. Note that this extra term influences only J_2 because $\mathbf{n} \cdot \mathbf{e}_1 = 0$ on Γ_C (for a straight crack[‡]).

[‡]Otherwise, \mathbf{e}_1 has to be defined as a variable along the crack faces [17].

4.2. Numerical evaluation of \mathbf{J}

As mentioned above, the extra boundary term in Equation (10) has not to be evaluated for J_1 . However, for J_2 the integration of the jump in the strain energy across the crack faces should be considered: this contribution does not vanish in general. In fact, the stress field near the crack tip can be expressed as

$$\begin{aligned}\sigma_{11} &= \frac{K_I}{\sqrt{2\pi r}} f_{11}^I(\theta) + \frac{K_{II}}{\sqrt{2\pi r}} f_{11}^{II}(\theta) + \sigma_{x0} + O(r^{1/2}) \\ \sigma_{22} &= \frac{K_I}{\sqrt{2\pi r}} f_{22}^I(\theta) + \frac{K_{II}}{\sqrt{2\pi r}} f_{22}^{II}(\theta) + O(r^{1/2}) \\ \sigma_{12} &= \frac{K_I}{\sqrt{2\pi r}} f_{12}^I(\theta) + \frac{K_{II}}{\sqrt{2\pi r}} f_{12}^{II}(\theta) + O(r^{1/2})\end{aligned}\quad (11)$$

where σ_{x0} is classically referred to as the T-stress [48]. Eischen [38] showed that, in this case, the jump in the strain energy is given by

$$\llbracket W \rrbracket(r)_{\text{crack faces}} = \frac{-4K_{II}\sigma_{x0}}{E^*\sqrt{r}} + O(r^{1/2}) \quad (12)$$

The jump will be zero only for pure mode I loading conditions ($K_{II}=0$) or for $\sigma_{x0}=0$. This also shows that the integration of the boundary term will be quite difficult because of its $1/\sqrt{r}$ behaviour. This is why various approaches have been proposed in order to accurately evaluate J_2 . The first proposal was given by Eischen and is developed in the following paragraph.

4.2.1. Accurate evaluation of J_2 : Eischen's proposal. Eischen [38] stated that the difficulties in the evaluation of J_2 is only due to the integration close to the crack tip. As the asymptotic behaviour of the mechanical fields is known in this region, he proposed to split the term into two integrals:

$$\int_{\Gamma_C} \llbracket W \rrbracket \mathbf{n} d\Gamma = \int_{\Gamma_C^*} \llbracket W \rrbracket \mathbf{n} d\Gamma + \int_{\Gamma_C^\delta} \llbracket W \rrbracket \mathbf{n} d\Gamma \quad (13)$$

where δ represents the length of the crack faces where the singular behaviour dominates: it defines two subsets of Γ_C (Γ_C^* and Γ_C^δ) as depicted in Figure 3. The author proposed to evaluate the first term of the right-hand side of Equation (13) by using the finite element approximation and the second term by considering the asymptotic energy jump (12). Then, Equation (13) becomes

$$\int_{\Gamma_C} \llbracket W \rrbracket \mathbf{n} d\Gamma = \int_{\Gamma_C^*} \llbracket W \rrbracket \mathbf{n} d\Gamma + \alpha \delta^{1/2} \quad (14)$$

where the multiplier α depends on the geometry of the problem, the loading conditions and the material moduli (i.e. α is invariant for a given problem). Eischen proposed to evaluate J_1 and J_2 considering two values of δ , i.e. δ_1 and δ_2 . Then, with three computations (J_1 , $J_2(\delta_1)$ and $J_2(\delta_2)$), it is possible to evaluate the stress intensity factors, the T-Stress and finally \mathbf{J} . This approach seems to lead to satisfactory results even for rather large values of δ . However, no convergence study was proposed in order to assess the accuracy of the method. Moreover, this approach is based on contour integrals that are not as accurate as domain integrals (see hereunder) for FEMs. A similar method with domain integrals was proposed by Chang and Yeh [40]; it is presented in the following section.

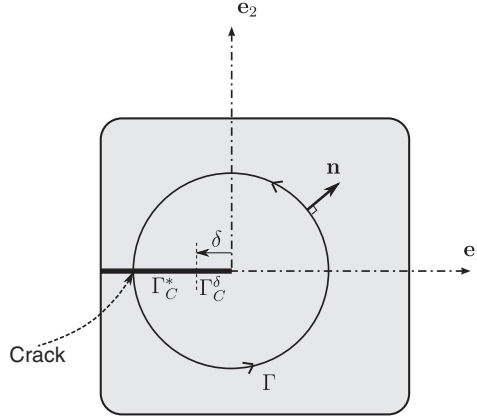


Figure 3. Definitions from [38].

4.2.2. *Accurate evaluation of J_2 : domain integral approach.* The domain integral method is a classical way to compute energy release rates within FEM and X-FEM. It was first introduced by Destuynder *et al.* [39] (see also Li *et al.* [49] and Shih *et al.* [50]). This method is very robust and has a convergence rate in $O(h)$, even with classical finite elements. The method introduces a virtual velocity field $\delta\mathbf{Q} = Q\mathbf{e}_1$, \mathbf{e}_1 being the unit vector tangent to the crack faces, and Q a sufficiently smooth scalar function, which equals 1 within Γ , and 0 on the contour Γ_e of the domain (see Figure 4 for the notations).

Then, the J -integral around Γ can be expressed in an equivalent domain form as

$$J = - \int_{\mathcal{V}} \underline{\nabla} \mathbf{Q} : \underline{\underline{M}} dV \quad (15)$$

where \mathcal{V} denotes the area between Γ_e and Γ , which is equal to the area inside Γ_e as Γ tends to zero. Following [40], this approach can be further extended to compute \mathbf{J} rather than J . In this case, two virtual velocity fields \mathbf{Q}_1 and \mathbf{Q}_2 are introduced

$$\mathbf{Q}_1 = \alpha \mathbf{e}_1 \text{ and } \mathbf{Q}_2 = \alpha \mathbf{e}_2 \text{ with } \alpha = 1 \text{ on } \Gamma \text{ and } \alpha = 0 \text{ on } \Gamma_e \quad (16)$$

Vector \mathbf{Q}_1 (resp. \mathbf{Q}_2) is tangent (resp. normal) to the crack faces. The k th component ($k=1, 2$) in the $(\mathbf{e}_1, \mathbf{e}_2)$ basis of the domain \mathbf{J} -integral is

$$J_k = \underbrace{\int_{\Gamma_C} \mathbf{Q}_k \cdot \llbracket W \rrbracket \cdot \mathbf{n} dA}_{J_k^B} - \underbrace{\int_{\mathcal{V}} \underline{\nabla} \mathbf{Q}_k : \underline{\underline{M}} dV}_{J_k^V} \quad \text{with } k=1, 2 \quad (17)$$

In this expression, the term J_k^B (resp. J_k^V) will be called a boundary term (resp. domain term) in the following. Note that the α weight function is chosen so that it is equal to 1 inside Γ and is equal to zero on Γ_e (plateau function). Finally, this approach can be easily extended to 3D problems [17]. The boundary term that appears in Equation (17)[§] is equivalent to that in Equation (10) and

[§]This term is also present for curved cracks.

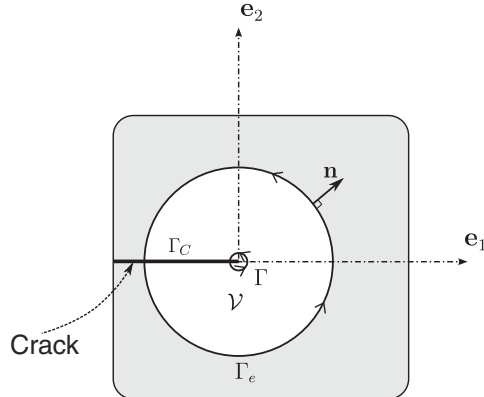


Figure 4. Definitions for the domain integral.

vanishes for the J_1 -integral but not for J_2 . The accuracy for the computation of the domain term J_2^V has been demonstrated both in the X-FEM and in the classical finite element context. Thus, the key issue for the calculation of the vectorial J -integral is the accuracy of the computation of the boundary term J_2^B . Chang and Yeh [40] proposed to proceed like Eischen, i.e. by splitting J_k^B into two parts. They considered the cases of both linear and non-linear elasticity. In the last case, a system of non-linear equations that results from the data set (geometry, loading conditions) with a number of different values of δ should be solved.

Here, we study the accuracy of the domain integral approach. However, we will not consider the previous works [38, 40], because we would like to evaluate \mathbf{J} without too many computations: two domain integrals, then the stress intensity factors and finally the \mathbf{J} -integral should be computed. If one wants to compute the \mathbf{J} -integral by means of the stress intensity factors, a simpler approach should consist in evaluating them directly using a domain interaction integral, which is known to be robust and accurate. Hence, we will directly evaluate Equation (15) similar to that by Heintz [41] who applied this approach in the context of enriched finite element approaches. In this work, the author derived a similar expression in the context of configurational mechanics. However, no convergence study was proposed so that the accuracy of the approach is not demonstrated. Moreover, no asymptotic enrichment was considered in the near-tip region, which means that the quality of the finite element fields may not be sufficient to evaluate J_k^B in a robust way (i.e. with accuracy, irrespective of the mesh topology).

4.3. Imprecisions with the domain integral approach

It has been shown that the evaluation of the domain \mathbf{J} -integral was leading to the sum of a domain term \mathbf{J}^V and a boundary term \mathbf{J}^B (Equation (17)). The latter term involves the integration of the energy jump across the crack faces. However, the energy evolves in r^{-1} near the crack tip (even if the jump follows an $r^{-1/2}$ evolution): if the r^{-1} terms do not vanish in the numerical evaluation of $\llbracket W \rrbracket$, the boundary term cannot be integrated.[¶] In this section, we first compare the errors due

[¶]As the integral between ε and 1 of $1/r$ does not converge when ε goes to zero.

to \mathbf{J}^V and \mathbf{J}^B using analytical fields and second exhibit the presence of spurious r^{-1} terms in \mathbf{J}^B when enriched finite element fields are considered.

Consider a 2×2 square-structured mesh of 882 triangular elements as depicted in Figure 8(a). This mesh is *fully enriched* with the near-tip basis Equation (6). The displacement field corresponding to a cracked plate in a mixed mode ($K_I = K_{II} = 1.0$, $E = 1.0 \text{ MPa}$, $\nu = 0$ and $\sigma_{x0} = 2.0$ in Equation (11)) is then projected onto the enriched finite element displacement field by means of an L^2 projection:

$$\int_{\Omega} \delta \mathbf{u}^h \cdot (\mathbf{u}^h - \mathbf{u}^{\text{exact}}) d\Omega = 0 \quad \forall \delta \mathbf{u}^h \quad (18)$$

As the exact solution field is contained in the enriched finite element approximation, the resulting numerical field exactly represents the analytical field. The \mathbf{J} -integral is then evaluated using a domain of radius 0.2. The errors due to the different terms of \mathbf{J} are summarized in Table I. The two components of \mathbf{J} can be accurately computed, especially J_1 . The presence of spurious r^{-1} terms is tested by changing the number of Gauss points for the integration of \mathbf{J}^B . If r^{-1} terms are still present in $\llbracket W \rrbracket$, then the value of J_2^B should degrade as the number of Gauss points increases. Figure 5 shows that J_2^B converges with a $O(n)$ rate (n being the number of Gauss points). This demonstrates that the computation of \mathbf{J} using domain integral is accurate when using mechanical fields of good quality. Next, the case where the mechanical field is obtained from a finite element solution is considered: the analytical stress field (Equation (11)) corresponding to the displacement

Table I. Integration error when \mathbf{J} is evaluated after L^2 projection of the analytical displacement field on the finite element displacement field (analytical value $J_1 = J_2 = 2.0$).

J_1 computed	Error	J_2^V computed	J_2^B computed	J_2 computed	Error
1.999757	0.01%	-3.389003	1.38271	-2.006292	0.31%

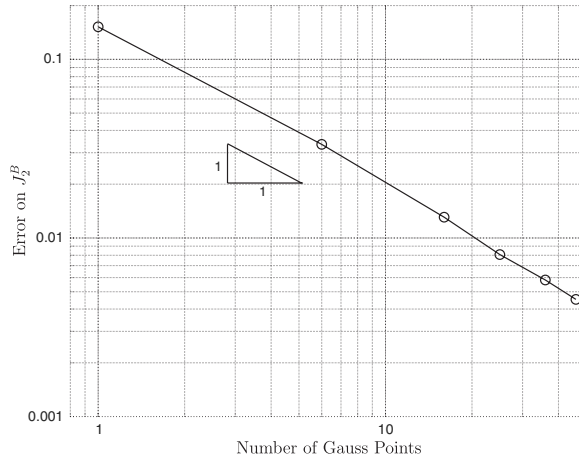


Figure 5. Convergence of J_2^B versus the number of Gauss points per element for a given mesh size (displacement field obtained using an L^2 projection).

Table II. Error partitionment when \mathbf{J} is computed using finite element fields.

J_1 computed	Error	J_2^V computed	Error	J_2^B computed	Error	J_2 computed	Error
1.970936	1.45%	-3.329226	1.76%	1.52225	10.09%	-1.806975	9.65%

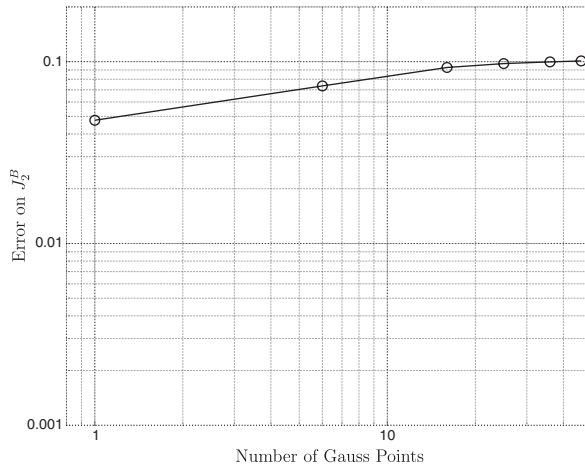


Figure 6. Convergence of J_2^B versus the number of Gauss points for a given mesh size (displacement field obtained by a finite element solution).

field used in the L^2 projection is applied on the boundary of the mesh and the problem is solved. The radius for the near-tip enrichment is set as 0.4 and \mathbf{J} is evaluated using the same domain radius (equal to 0.2) as in the projection. Table II shows that the degradation in the accuracy of J_1 is small, whereas it is huge for J_2 , and that this degradation is mainly due to the boundary term J_2^B . Finally, the convergence of J_2^B with respect to the number of Gauss points shows that J_2^B does not converge to its exact value, either because of the quality of the mechanical fields or because of the remaining spurious r^{-1} terms (see Figure 6). We can then conclude that the imprecision in the computation of J_2^B is a consequence of a global lack of quality in the finite element solution. However, it is still not clear whether convergence can be obtained using finite element fields.

5. ROBUST EVALUATION OF THE VECTORIAL J-INTEGRAL

5.1. Improvement in accuracy and robustness for the computation of \mathbf{J}

An alternative approach is proposed for the evaluation of the \mathbf{J} -integral at the crack tip. Equation (17) shows that the computation of J_2^B leads to the integration of the energy jump between the crack faces. As shown in Equation (12), this term vanishes if the (regular) T-stress σ_{x0} is zero. Moreover, if the T-stress can be computed, then the boundary term of the domain integral vanishes if the regular stress field $\sigma_{x0}\mathbf{e}_1 \otimes \mathbf{e}_1$ is subtracted from the singular stress field (see Equations (11)). This operation does not change the value of the \mathbf{J} -integral [48], but allows one to remove the boundary

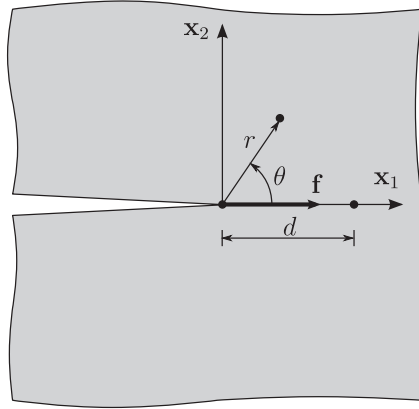


Figure 7. Concentrated force $\mathbf{f} = f \mathbf{e}_1$ applied at the crack tip of a cracked semi-infinite body.

term from Equation (17). The T-stress can be evaluated using a path-independent interaction integral I^{A+B} [51]:

$$I^{A+B} = \int_{\gamma} (\sigma_{ij}^A u_{i,1}^B + \sigma_{ij}^B u_{i,1}^A - \sigma_{ik}^A \varepsilon_{ik}^B \delta_{1j}) q_{,j} dS \quad (19)$$

where the superscript A denotes the finite element field and the superscript B denotes an auxiliary field as originally proposed by Michell [52]. This auxiliary field corresponds to the analytical solution to an infinite cracked plate loaded at its tip by a force $\mathbf{f} = f \mathbf{e}_1$ (see Figure 7). Sladek and Sladek [51] have shown that the interaction integral Equation (19) is related to the T-stress by

$$I^{A+B} = \frac{T}{E^*} f \quad (20)$$

where $E^* = E/(1-\nu^2)$ and $E^* = E$ for plane strain and plane stress problems, respectively. After having determined the T-stress, the \mathbf{J} -integral can be evaluated using only domain integrals and without considering the boundary term, which is the major source of error.

5.2. Convergence study

The convergence of the two domain approaches presented above is now studied by considering the cracked domain $\Omega = [-1, 1] \times [-1, 1]$ under tension as shown in Figure 8. Tensions applied on domain boundaries are the tensions corresponding to the problem of an infinite cracked body under a mixed mode (using the analytical solution Equation (11) with $K_I = 1.0$ and $K_{II} = 1.0$). The material properties are Young's modulus $E = 1.0$ and Poisson's ratio $\nu = 0.3$. A sequence of gradually refined meshes is considered: those meshes are defined so that the crack always passes through finite elements (see Figure 8(a) for a typical mesh). Two different enrichment methods are considered for the near-tip region: first, no near-tip enrichment (only the Heaviside function is considered); second, the so-called 'geometrical' enrichment recently introduced in [42, 45, 53] is adopted. In the latter case, all nodes lying in a disk (of radius 0.1 here) are enriched with near-tip fields. The authors have established numerically that the convergence rate in the energy

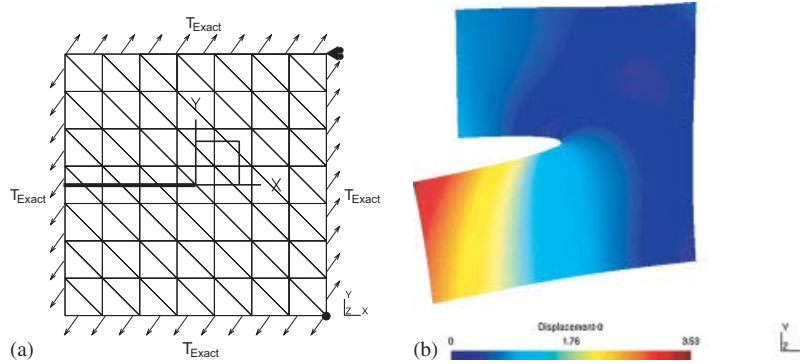


Figure 8. (a) Domain of interest and (b) deformed shape for $K_I=1.0$ and $K_{II}=1.0$.

norm is improved from $O(h^{1/2})$ to $O(h)$ for a given benchmark.^{||} Here, this geometrical approach is applied to study the convergence of \mathbf{J} at the crack tip and to exhibit the influence of the boundary term on the computation of domain integrals. Stress intensity factors are prescribed so that analytical values of J_1 and J_2 are known [54]:

$$J_1 = \frac{K_I^2 + K_{II}^2}{E^*} \quad (21)$$

$$J_2 = -2 \frac{K_I K_{II}}{E^*} \quad (22)$$

with $E^* = E/(1-\nu^2)$ and $E^* = E$ for plane strain and plane stress problems, respectively.

The T-stress σ_{x0} is set to as 2.0 (the boundary term is then non-zero in Equation (17)), and the convergence study is performed using a domain of radius 0.2 for the computation of domain integrals. Four cases are considered:

1. domain integral method (radius 0.2) using X-FEM without near-tip enrichment (the crack tip ends on the edge of an element);
2. domain integral method (radius 0.2) using X-FEM and geometrical near-tip enrichment (radius 0.1, basis given by (6));
3. T-stress method (radius 0.2) using X-FEM without near-tip enrichment;
4. T-stress method (radius 0.2) using X-FEM and geometrical (radius 0.1) near-tip enrichment.

The first and second cases allow one to study the influence of the quality of the finite element field on the convergence properties of the domain integral method. The results are presented in Figure 9.

As shown in Figure 9(a), the first component of \mathbf{J} , J_1 converges at the expected rate [42, 45], i.e. $O(h^2)$ for the geometrical enrichment. Concerning J_2 , there is no convergence if the boundary term J_2^B is not taken into account (see the curve labeled ' J_2 Domain Integral X-FEM Geometrical (w/o Bnd Term)' in Figure 9(b)). When this term is taken into account, convergence (rate $O(h)$) is obtained only if near-tip enrichment is considered: the quality of the finite element fields is not sufficient without near-tip enrichment to ensure convergence (see the curve labeled ' J_2 Domain

^{||}Note that this convergence improvement was not proved mathematically.

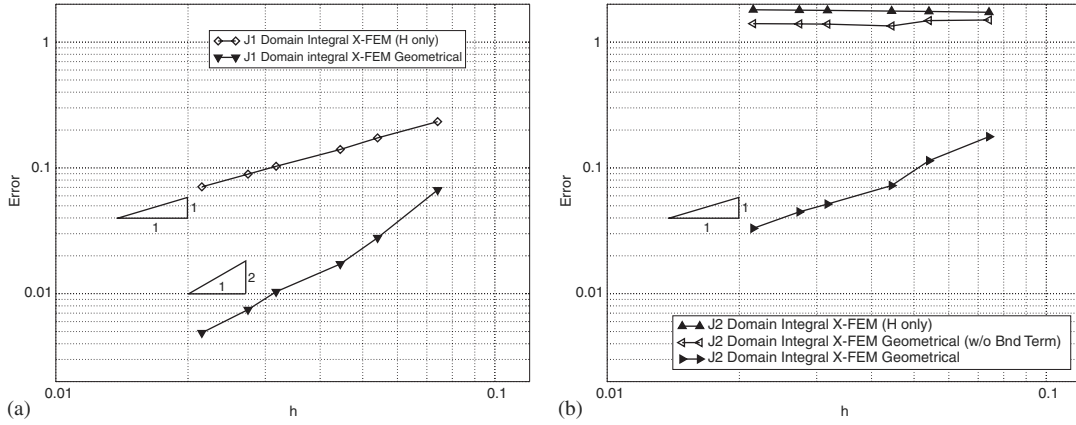


Figure 9. Convergence for $K_I=1.0$, $K_{II}=1.0$ and $\sigma_{x0}=2.0$: (a) J_1 component and (b) J_2 component. Curves ‘ J_k Domain Integral X-FEM (H only)’ stand for X-FEM computations of J_k ($k=1, 2$) without near-tip enrichment (the crack tip ends on the edge of an element), and taking into account the boundary term J_2^B . Curves ‘ J_k Domain Integral X-FEM Geometrical’ stand for X-FEM computations of J_k ($k=1, 2$) with geometrical near-tip enrichment, and taking into account the boundary term J_2^B . Curve ‘ J_2 Domain Integral X-FEM Geometrical (w/o Bnd Term)’ stands for X-FEM computations of J_2 with geometrical near-tip enrichment, and *without* taking into account the boundary term J_2^B .

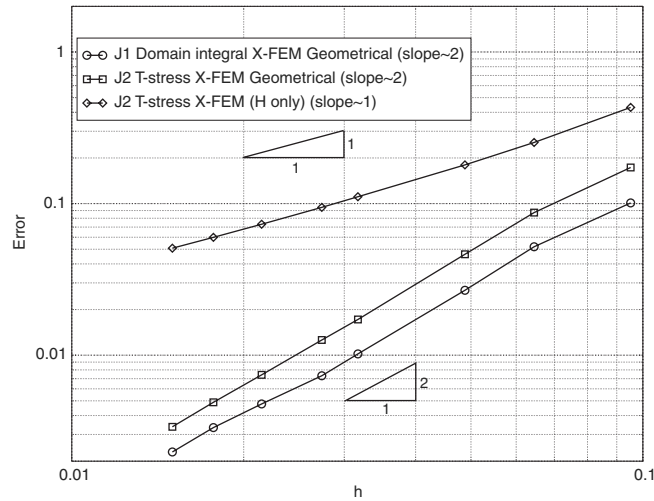


Figure 10. Interaction integral method: convergence for $K_I=1.0$, $K_{II}=1.0$ and $\sigma_{x0}=2.0$.

Integral X-FEM (H only)). In fact, this last computational setting corresponds to the one used in [41]. Finally, even with near-tip enrichment, convergence rates are different for the two components of the \mathbf{J} -integral: it is optimal for J_1 but not for J_2 .

Consider now the convergence of the method proposed in Section 5.1 as presented in Figure 10. It is seen now that both J_1 and J_2 converge at the same rate ($O(h^2)$) with a very low error level

Table III. Summary of the convergence rates of J_k -integrals.

	Geometrical domain integral X-FEM	Geometrical domain integral +bnd term X-FEM	Geometrical T-stress domain integral X-FEM
J_1	$O(h^2)$	$O(h^2)$	$O(h^2)$
J_2	—	$O(h)$	$O(h^2)$

even for coarse meshes. The figure also shows that convergence is obtained even without near-tip enrichment, which was not the case with the classical domain integrals. Results obtained with this benchmark are summarized in Table III, and they clearly exhibit the accuracy of the proposed approach.

6. CONCLUSION

In this paper, the accuracy of the numerical computation of path-independent J_k -integrals using domain integrals has been investigated. It has been recalled that a boundary term (related to the near-tip stress field) had to be considered to evaluate these quantities. However, the lack of accuracy of the numerical scheme adopted for the integration of this boundary term can lead to a loss of convergence. In particular, J_k -domain integrals do not converge without near-tip enrichment (contrary to what was assumed in [41]). Moreover, even if it converges, optimal rate cannot be obtained for J_2 . To overcome these limitations, an alternative approach based on the evaluation of the T-Stress has been proposed to avoid the integration of the boundary term. In this case, optimal rates of convergence are recovered for J_2 . However, this paper considered only the linear-elastic bi-dimensional case. Investigations are still needed to extend these results to non-linear elastic-plastic fracture, and to the 3D setting. In the latter case, the T-stress is no longer scalar, but becomes a vectorial parameter, which leads to some extra difficulties. In addition, it is important to note that the results presented here imply consequences in the context of configurational mechanics [55] (for generalities on this theory, see Gurtin [56], Maugin [57, 58] and Steinmann [59, 60] among others). As a matter of fact, it can be shown (see Appendix A) that nodal configurational forces, introduced by Steinmann [59, 60], are similar to the domain \mathbf{J} -integral on the support of the node that contains the crack tip, but without the boundary term, which is mandatory for convergence. Thus, nodal configurational forces cannot converge to \mathbf{J} .

APPENDIX A: RELATIONSHIP BETWEEN DOMAIN \mathbf{J} -INTEGRAL AND NODAL CONFIGURATIONAL FORCES

Recall the expression of the k th component of the nodal material force acting on node I as depicted in Figure A1 [59]:

$$\mathcal{F}_k^s = \bigcup_{e=1}^{N_{\text{Elem}}} \int_{\Omega_e} (\underline{\underline{\mathbf{M}}}: \underline{\underline{\nabla}} \mathbf{N}^k) dV \quad (\text{A1})$$

where N_{Elem} is the number of elements connected to node I. Next, we consider the k th component of the domain \mathbf{J} -integral (without the boundary term) expressed on the support (denoted as \mathcal{V}_I)

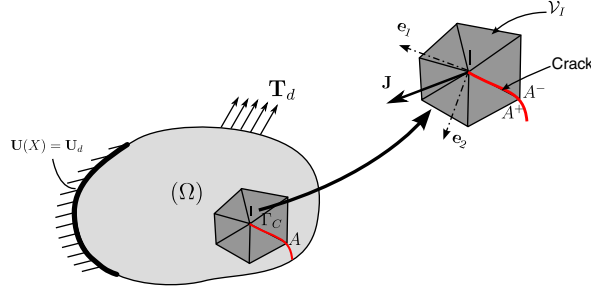


Figure A1. Configurational force acting on node I and support of the node.

of node I

$$J_k^V = - \int_{\mathcal{V}_I} \underline{\nabla} \mathbf{Q}_k : \underline{\underline{M}} dV \quad (\text{A2})$$

where the plateau test function is interpolated using the finite element shape functions

$$\mathbf{Q}_k = \sum_{n=1}^{N_{\text{nodes}}} \alpha_n N^n \mathbf{e}_k \quad (\text{A3})$$

with N_{nodes} being the number of nodes on the support of node I. Then, we have

$$J_k^V = - \sum_{n=1}^{N_{\text{nodes}}} \alpha_n \int_{\mathcal{V}_I} \underline{\nabla} (N^n \mathbf{e}_k) : \underline{\underline{M}} dV \quad (\text{A4})$$

The only way to prescribe $\alpha=1$ at crack tip and $\alpha=0$ on the contour of \mathcal{V}_I is to set all $(\alpha_n)_{n>1}$ to zero and $\alpha_1=1$. Thus, Equation (A4) becomes

$$J_k^V = - \int_{\mathcal{V}_I} \underline{\nabla} (N^1 \mathbf{e}_k) : \underline{\underline{M}} dV = - \bigcup_{e=1}^{N_{\text{Elem}}} \int_{\Omega_e} \underline{\nabla} \mathbf{N}^k : \underline{\underline{M}} dV \quad (\text{A5})$$

Simply comparing Equations (A1) and (A5), we have $J_k^V = -\mathcal{F}_k^s$. This demonstrates that the nodal configurational force is not the \mathbf{J} -integral, because the boundary term J_k^B is missing (see Equation (17)).

This missing term corresponds to a configurational Neumann boundary condition on Γ_C : this boundary condition should not vanish as a traction-free surface in the physical space does not lead to a configurational-free surface.

REFERENCES

1. Lu YY, Belytschko T, Gu L. Element-free Galerkin methods. *International Journal for Numerical Methods in Engineering* 1994; **51**:221–258.
2. Duarte C, Oden J. An hp meshless method. *Numerical Methods for Partial Differential Equations* 1996; **12**: 673–705.
3. Babuska I, Melenk JY. The partition of unity finite element method. *International Journal for Numerical Methods in Engineering* 1997; **40**(4):727–758.

4. Duarte CA, Oden JT. An h-p adaptive method using clouds. *Computer Methods in Applied Mechanics and Engineering* 1996; **139**(1-4):237–262.
5. Strouboulis T, Babuška I, Copps K. The design and analysis of the generalized finite element method. *Computer Methods in Applied Mechanics and Engineering* 2000; **181**:43–69.
6. Strouboulis T, Copps K, Babuška I. The generalized finite element method. *Computer Methods in Applied Mechanics and Engineering* 2001; **190**(32–33):4081–4193.
7. Duarte CA, Babuška I, Oden JT. Generalized finite element methods for three-dimensional structural mechanics problems. *Computers and Structures* 2000; **77**(2):215–232.
8. Oden JT, Duarte CAM, Zienkiewicz OC. A new cloud-based hp finite element method. *Communications in Numerical Methods in Engineering* 1998; **153**(1–2):117–126.
9. Strouboulis T, Zhang L, Babuška I. Generalized finite element method using mesh-based handbooks: application to problems in domains with many voids. *Computer Methods in Applied Mechanics and Engineering* 2003; **192**:3109–3161.
10. Strouboulis T, Zhang L, Babuška I. p-Version of the generalized FEM using mesh-based handbooks with applications to multiscale problems. *International Journal for Numerical Methods in Engineering* 2004; **60**(10):1639–1672.
11. Belytschko T, Black T. Elastic crack growth in finite elements with minimal remeshing. *International Journal for Numerical Methods in Engineering* 1999; **45**(5):601–620.
12. Moës N, Dolbow J, Belytschko T. A finite element method for crack growth without remeshing. *International Journal for Numerical Methods in Engineering* 1999; **46**:131–150.
13. Sukumar N, Huang ZY, Prévost JH, Suo Z. Partition of unity enrichment for bimaterial interfacial cracks. *International Journal for Numerical Methods in Engineering* 2004; **59**:1075–1102.
14. Budyn E, Zi G, Moës N, Belytschko T. A method for multiple crack growth in brittle materials without remeshing. *International Journal for Numerical Methods in Engineering* 2004; **61**:1741–1770.
15. Legrain G, Moës N, Huerta A. Stability of incompressible formulations enriched with X-FEM. *Computer Methods in Applied Mechanics and Engineering* 2008; **197**:1835–1849.
16. Xiao QZ, Karihaloo BL. Direct evaluation of accurate coefficients of the linear elastic crack tip asymptotic field. *Fatigue and Fracture of Engineering Materials and Structures* 2003; **26**(8):719–729.
17. Moës N, Gravouil A, Belytschko T. Non-planar 3D crack growth by the extended finite element and level sets. Part I: mechanical model. *International Journal for Numerical Methods in Engineering* 2002; **53**:2549–2568.
18. Gravouil A, Moës N, Belytschko T. Non-planar 3D crack growth by the extended finite element and level sets. Part II: level set update. *International Journal for Numerical Methods in Engineering* 2002; **53**:2569–2586.
19. Sukumar N, Moës N, Belytschko T, Moran B. Extended finite element method for three-dimensional crack modelling. *International Journal for Numerical Methods in Engineering* 2000; **48**(11):1549–1570.
20. Bordas S, Moran B. Enriched finite elements and level sets for damage tolerance assessment of complex structures. *Engineering Fracture Mechanics* 2006; **73**(9):1176–1201.
21. Dolbow J, Moës N, Belytschko T. An extended finite element method for modeling crack growth with frictional contact. *Computer Methods in Applied Mechanics and Engineering* 2001; **190**:6825–6846.
22. Dolbow J, Moës N, Belytschko T. Modeling fracture in Mindlin–Reissner plates with the eXtended finite element method. *International Journal of Solids and Structures* 2000; **37**:7161–7183.
23. Wyart E, Coulon D, Duflo M, Pardo T, Remacle J-F, Lani F. A substructured FE-shell/XFE-3D method for crack analysis in thin-walled structures. *International Journal for Numerical Methods in Engineering* 2007; **72**(7):757–779.
24. Moës N, Belytschko T. Extended finite element method for cohesive crack growth. *Engineering Fracture Mechanics* 2002; **69**:813–834.
25. Wells GN, Sluys LJ. A new method for modelling cohesive cracks using finite elements. *International Journal for Numerical Methods in Engineering* 2001; **50**:2667–2682.
26. Réthoré J, Gravouil A, Combescure A. An energy-conserving scheme for dynamic crack growth using the eXtended finite element method. *International Journal for Numerical Methods in Engineering* 2005; **53**:2569–2586.
27. Dolbow JE, Devan A. Enrichment of enhanced assumed strain approximations for representing strong discontinuities: addressing volumetric incompressibility and the discontinuous patch test. *International Journal for Numerical Methods in Engineering* 2004; **59**:47–67.
28. Legrain G, Moës N, Verron E. Stress analysis around crack tips in finite strain problems using the eXtended finite element method. *International Journal for Numerical Methods in Engineering* 2005; **63**:290–314.
29. Areias PMA, Belytschko T. Analysis of three-dimensional crack initiation and propagation using the extended finite element method. *International Journal for Numerical Methods in Engineering* 2005; **63**(5):760–788.

30. Gasser TT, Holzapfel GA. Geometrically non-linear and consistently linearized embedded strong discontinuity models for 3D problems with an application to the dissection analysis of soft biological tissues. *Computer Methods in Applied Mechanics and Engineering* 2003; **192**(47–48):5059–5098.
31. Mergheim J, Kuhl E, Steinmann P. Towards the algorithmic treatment of 3D strong discontinuities. *Communications in Numerical Methods in Engineering* 2006; **23**:97–108.
32. Karihaloo BL, Xiao QZ. Modelling of stationary and growing cracks in FE framework without remeshing: a state-of-the-art review. *Computers and Structures* 2003; **81**:119–129.
33. Erdogan F, Sih GC. On the crack extension in plates under plane loading and transversal shear. *Journal of Basic Engineering* 1963; **85**:519–527.
34. Leblond JB. Crack paths in plane situations. I: general form of the expansion of the stress intensity factors. *International Journal of Solids and Structures* 1989; **25**(11):1311–1325.
35. Ma L, Korsunsky AM. On the use of the vectorial j-integral in crack growth criteria for brittle solids. *International Journal of Fracture* 2005; **133**:39–46.
36. Hellen TK, Blackburn WS. The calculation of stress intensity factors for combined tensile and shear loading. *International Journal of Fracture* 1975; **11**:605–617.
37. Herrmann AG, Herrmann G. On energy release rates for a plane crack. *Journal of Applied Mechanics* 1981; **48**:525–528.
38. Eischen JW. An improved method for computing the J2 integral. *Engineering Fracture Mechanics* 1987; **26**(5):691–700.
39. Destuynder Ph, Djaoua M, Lescure S. Quelques remarques sur la mécanique de la rupture élastique. *Journal de mécanique théorique et appliquée* 1983; **2**(1):113–135.
40. Chang JH, Yeh JB. Calculation of j2-integral of 2D cracks in rubbery materials. *Engineering Fracture Mechanics* 1998; **59**(5):683–695.
41. Heintz P. On the numerical modelling of quasi-static crack growth in linear elastic fracture mechanics. *International Journal for Numerical Methods in Engineering* 2006; **62**(2):174–189.
42. Béchet E, Minnebo H, Moës N, Burgardt B. Improved implementation and robustness study of the X-FEM for stress analysis around cracks. *International Journal for Numerical Methods in Engineering* 2005; **64**(8):1033–1056.
43. Stolarska M, Chopp DL, Moës N, Belytschko T. Modelling crack growth by level sets and the extended finite element method. *International Journal for Numerical Methods in Engineering* 2001; **51**(8):943–960.
44. Chopp DL, Sukumar N. Fatigue crack propagation of multiple coplanar cracks with the coupled extended finite element/fast marching method. *International Journal of Engineering Science* 2003; **41**:845–869.
45. Laborde P, Pommier J, Renard Y, Salaün M. High-order extended finite element method for cracked domains. *International Journal for Numerical Methods in Engineering* 2005; **64**(3):354–381.
46. Rice J. A path independent integral and the approximation analysis of strain concentration by notches and cracks. *Journal of Applied Mechanics* 1968; **35**:379–386.
47. Eshelby JD. The force on an elastic singularity. *Philosophical Transactions of the Royal Society of London, Series A* 1951; **244**:87–112.
48. Rice JR. Limitations to the small scale yielding approximation for crack tip plasticity. *Journal of Mechanics and Physics of Solids* 1974; **22**:17–26.
49. Li FZ, Shih CF, Needleman A. A comparison of methods for calculating energy release rates. *Engineering Fracture Mechanics* 1985; **21**:405–421.
50. Shih CF, Moran B, Nakamura T. Energy release rate along a three-dimensional crack front in a thermally stressed body. *International Journal of Fracture* 1986; **30**:79–102.
51. Sladek J, Sladek V. Evaluation of T-stresses and intensity factors in stationary thermoelasticity by the conservation integral method. *International Journal of Fracture* 1997; **86**:199–219.
52. Michell JH. Elementary distributions of plane stress. *Proceedings of the Royal Mathematical Society of London* 1900; **32**:35–61.
53. Chahine E, Laborde P, Renard Y. A quasi-optimal convergence result for fracture mechanics with XFEM. *Comptes Rendus Mathématique* 2006; **342**(7):527–532.
54. Bui HD. *Mécanique de la rupture fragile*. Masson: Paris, 1978.
55. Eshelby JD. The elastic energy–momentum tensor. *Journal of Elasticity* 1975; **5**(3–4):321–335.
56. Gurtin ME. *Configurational Forces as Basic Concepts of Continuum Physics*. Springer: Berlin, 1999.
57. Mueller R, Maugin GA. On material forces and finite element discretizations. *Computational Mechanics* 2002; **29**:52–60.

58. Maugin GA, Trimarco C. Pseudomomentum and material forces in nonlinear elasticity. Variational formulations and application to brittle fracture. *Acta Mechanica* 1992; **94**(1-2):1-28.
59. Steinmann P, Ackermann D, Barth FJ. Application of material forces to hyperelastostatic fracture mechanics. II. Computational setting. *International Journal of Solids and Structures* 2001; **38**:5509-5526.
60. Steinmann P. Application of material forces to hyperelastostatic fracture mechanics. I. Continuum mechanical setting. *International Journal of Solids and Structures* 2000; **37**:7371-7391.